Biometals (2010) 23:1075–1084
DOI 10.1007/s10534-010-9353-x

From GC-rich DNA binding to the repression of survivin gene for quercetin nickel (II) complex: implications for cancer therapy

Jun Tan · Liancai Zhu · Bochu Wang

Received: 5 December 2009 / Accepted: 31 May 2010 / Published online: 25 June 2010

Abstract The DNA binding and cleavage properties of quercetin nickel (II) complex have been studied, but little attention has been devoted to the relationship between antitumor activity of this complex and DNA-binding properties. In the present study, we report that quercetin nickel (II) complex showed significant cytotoxicity against three tumor cell lines (HepG2, SMMC7721 and A549). Hoechst33258 and AO/EB staining showed HepG2 cells underwent the typical morphologic changes of apoptosis characterized by nuclear shrinkage, chromatin condensation, or fragmentation after exposure to quercetin nickel (II) complex. We also demonstrate that the levels of survivin and bcl-2 protein expression in HepG2 cells decreased concurrently, and the levels of p53 protein increased significantly after treatment with quercetin nickel (II) complex by immunocytochemistry analysis. The relative activity of caspase-3 and caspase-9 increased significantly after treatment with the complex. Furthermore, fluorescence measurements and molecular modeling were performed to learn that the complex could be preferentially bound to DNA in GC region. These results imply that quercetin nickel (II) complex may intercalate into the GC-rich core promoter region of survivin, down-regulating survivin gene expression and promoting tumor cells apoptosis. So our results suggest that antitumor activity of quercetin nickel (II) complex might be related to its intercalation into DNA and DNA-binding selectivity, and that the complex may be a promising agent for cancer therapy.

Keywords Quercetin nickel (II) complex · Selective DNA binding · Antitumor activity · Survivin · GC-rich

Electronic supplementary material The online version of this article (doi:10.1007/s10534-010-9353-x) contains supplementary material, which is available to authorized users.

J. Tan (✉) · L. Zhu · B. Wang (✉)
Key Laboratory of Biorheological Science and Technology, Ministry of Education, Bioengineering College, Chongqing University, No. 174, Shapingba Main Street, Chongqing 400030, China
e-mail: tanjunmail@126.com

J. Tan
Department of Life Science & Chemistry, Chongqing Education College, Chongqing 400067, China

J. Tan
Post-Doctoral Research Center of Mechanics, Mechanical Resource and Environment College, Chongqing University, Chongqing 400030, China

Introduction

In recent years, many research have been focused on the interaction of small molecules with DNA (Song et al. 2006; Kožurková et al. 2008; Tan et al. 2008). DNA is generally the primary intracellular target of anticancer drugs, because the interaction between

small molecules and DNA can cause DNA damage in cancer cells, blocking the division of cancer cells and resulting in cell death (Zuber et al. 1998; Hecht 2000; Sastry and Patel 1993). Particularly, some compounds preferentially binding to GC-rich DNA are able to block overactive transcription factors and modulate gene expression, which could be very attractive therapeutic agents. Some anticancer antibiotics, such as mithramycin and hedamycin, have the interesting property of binding to GC-rich DNA sequences selectively (Sastry and Patel 1993; Wu et al. 2005), because the chromophores form specific hydrogen bonds with the NH_2 of guanines (Sastry and Patel 1993; Sastry et al. 1995). As consequence of this sequence selectivity, mithramycin blocks the binding of the specificity protein 1 (Sp1) family of transcription factors to CG-rich DNA sequences in gene promoters and inhibits gene transcription, which in turn alters the regulation of cell proliferation and differentiation (Ray et al. 1990; Remsing et al. 2003; Albertini et al. 2006; Koutsodontis and Kardassis 2004). Among these genes, survivin has recently appeared to be an attractive cancer therapeutic target because it is selectively expressed in most tumor cells and it is required for their viability (Altieri 2001). It has been demonstrated that the specific interactions of Sp1 or Sp1-like proteins with the cis-acting DNA elements in GC-rich human survivin promoter are of great importance for its basal transcription, and that the inhibition of these interactions by the anticancer agent could down-regulate survivin transcription (Wu et al. 2005).

In addition, there is a great interest on the binding of metal complexes with DNA, owing to their possible applications as new cancer therapeutic agents (Metcalfe and Thomas 2003; Silvestri et al. 2004; Navarro et al. 2003; Zhang et al. 2005; Sheng et al. 2008). It has been reported that the DNA-binding ability of a complex was involved in the planarity of ligand, the coordination geometry, ligand donor atom type and the metal ion type (Xu et al. 2003a, b; Asadi et al. 2004). Among these complexes, some metal complexes such as ruthenium (II) polypyridyl complexes preferentially bind to GC sequences in the DNA (Gao et al. 2008), and quercetin metal complexes could cleave the pBR322 DNA (Tan et al. 2007a, b). Especially, flavonoids such as quercetin can slightly bind to DNA, but quercetin metal complexes which quercetin chelates metal ions to form exhibit stronger DNA-binding affinities than quercetin alone (Tan et al. 2009a, b, c). However, little is known about the relation between their DNA-binding selectivity and regulation of gene expression.

In this study, the DNA-binding selectivity and apoptosis-inducing activity of quercetin nickel (II) complex were investigated. We demonstrate that the antitumor mechanism of quercetin nickel (II) complex could be involved in not only its down-regulation of survivin gene, but also its specific interaction with DNA.

Materials and methods

Materials

All chemicals and reagents were purchased from commercial sources and were used without further purification. Quercetin (Que), 3-(4,5-dimethylthiazol-2-yl)-2,5-diphenyl-2*H*-tetrazolium bromide (MTT), Hoechst33258, acridine orange (AO), ethidium bromide (EB), calf thymus DNA (CT DNA), poly(dA)·poly(dT) and poly(dG)·poly(dC) were obtained from Sigma. The Tris–HCl buffer solution was prepared with triple distilled water. Anti-survivin (ZM-0468), anti-bcl-2 (ZM-0010) and anti-p53 (ZM-0408) were purchased from Santa Cruz Biotechnology. SP-9000 Histostain^{TM}-Plus kits were from Zymed Laboratories. Caspase-3, 8 and 9 colorimetric assay kits were from Nanjing Keygen Biotech. Co. The structure of quercetin nickel (II) complex, $Ni(Que)_2(H_2O)_2$, was reported in our previous study (Tan et al. 2009c). Each Ni (II) ion coordinates carbonyl oxygen, hydroxy oxygen atoms of quercetin and oxygen atoms of H_2O.

Cell culture

Human hepatocellular liver carcinoma (HepG2), human hepatoma (SMMC7721) and human lung adenocarcinoma (A549) cell lines were obtained from the American Type Culture Collection. The three cell lines were cultured in RPMI 1640 medium supplemented with 10% fetal bovine serum, 100 units/ml penicillin, 100 μg/ml streptomycin, L-glutamine (0.03%, w/v), and sodium bicarbonate (2.2%, w/v). Cell cultures were kept in a humidified incubator with 5% CO_2 at 37°C. And subcultures

were performed with 0.05% trypsin–0.02% EDTA in phosphate-buffered saline (PBS).

Cytotoxicity evaluation

The cytotoxicity or survival of cells in the presence or absence of the experimental agent was determined using a system based on MTT as described previously (Mosmann 1983). The tumor cells (HepG2, SMMC7721 and A549) were plated into 96-well microtiter plates at a density of 1×10^4 cells per well. After 24 h, culture medium was replaced by 200 μl RPMI 1640 medium supplemented with 10% fetal bovine serum in the presence of various concentrations (0, 6.25, 12.5, 25, 50 and 100 μM) of $Ni(Que)_2(H_2O)_2$ complex or $(Que)_2$ (its concentration was calculated as two molecules), and the cells were incubated for 24, 48 and 72 h. The final concentration of solvent was less than 0.1% in cell culture medium. Culture solutions were removed and replaced by 90 μl culture medium. Ten microliters of sterile filtered MTT solution (5 mg/ml) in PBS (pH 7.4) was added to each well reaching a final concentration of 0.5 mg MTT/ml. Then cells were incubated at 37°C for 4 h. After the medium and unreacted dye had been removed, DMSO (200 μl) was added to each well. The absorbance at 490 nm of the dissolved solution was measured with a Bio-Rad 680 microplate reader. The relative cell viability (percent, %) related to control wells containing cell culture medium without the compound tested was calculated by dividing the absorbance of the treated cells by that of the control in each experiment. The IC_{50} value was calculated using SPSS statistical software as the concentration of the compound tested which inhibits growth of 50% of cells relative to nontreated control cells.

Apoptosis assessment by Hoechst33258 and AO/EB staining

Chromatin condensation was detected by nuclear staining with Hoechst33258. The HepG2 cells were cultured on cover slips, which were kept in a 60 Petri dish for 24 h before treatment. After treatment with 0, 40 or 80 μM $Ni(Que)_2(H_2O)_2$ complex for 24 h, HepG2 cells were fixed with ice-cold methanol and acetic acid (3:1) at room temperature for 5 min and exposed to Hoechest33258 staining solution (5 μg/ml) at room temperature in the dark for 15 min. Samples were observed under a fluorescence microscope (Olympus BX-51, Japan). For AO/EB staining, the cells without fixation were loaded with a 100 μl fresh-prepared AO/EB staining solution (100 μg/ml), then immediately observed under a fluorescence microscope in less than 20 min.

Immunocytochemistry analysis

The cells were cultured on cover slips, which were kept in a 60 Petri dish for 24 h before treatment. After treatment with 0, 20 or 60 μM $Ni(Que)_2(H_2O)_2$ complex for 24 h, the cells were washed three times with isotonic PBS (pH 7.4) and then fixed in 4% paraformaldehyde solution in PBS for 15 min at 37°C. Then the cells were washed three times with PBS (pH 7.4) and incubated with 0.3% Triton X-100 in PBS for 20 min at 37°C. The slides were immersed in 3% H_2O_2 in methanol at 20°C for 15 min to block endogenous peroxidase activity. Then the cover slips were washed three times with PBS, and nonspecific binding sites were blocked in PBS containing 10% normal goat serum for 30 min. The cells were incubated with rabbit anti-human surviving, mouse anti-human bcl-2, or mouse anti-human p53 antibody (1:100) in PBS containing 10% normal goat serum overnight at 4°C and washed three times with PBS. Then the cells were incubated with biotin-conjugated goat anti-rabbit/-mouse IgG in PBS containing 10% normal goat serum for 40 min at 37°C and washed three times with PBS. The cells were incubated with horseradish peroxidase labeled streptavidin in PBS for 60 min at 37°C. After the slides had been washed three times, horseradish peroxidase was visualized by freshly prepared 3,3′-diamino-benzidine tetrahydrochloride (DAB)/H_2O_2 in the dark for 10 min. The coloring reaction was stopped by washing the slides with water and then the nuclei were counterstained with Mayer's hematoxylin for 1 min. Finally, the slides were dehydrated with ethanol, cover-slipped with DPX, observed and photographed with an Olympus optical microscope.

Negative controls in which the primary antibody was omitted and positive controls for each antibody were included in each batch of immunocytochemistry.

Determination of caspase activity by absorption spectroscopy

The measurement of caspase-3, -8, and -9 activities was performed using a caspase colorimetric protease assay kits. The HepG2 cells were plated at a density of 1×10^6 cells per well in complete RPMI 1640 medium for 24 h. After treatment with 0, 20 or 60 μM $Ni(Que)_2(H_2O)_2$ complex for 24 h, cells were harvested and washed three times with cold PBS by centrifugation (1,000×*g*, 3 min) to stop the incubation. Cells were resuspended in 50 μl of chilled cell lysis buffer containing *N*-(2-hydroxyethyl)piperazine-*N*′-ethanesulfonic acid (50 mM, pH 7.4), 3-[(3-cholamidopropyl)dimethylammonio]propanesulfonate (5 mM), and dithiothreitol (5 mM). After they had been incubated on ice for 10 min, and centrifuged for 1 min in a microcentrifuge (10,000×*g*), the supernatants (cytosolic extract) were transferred to a fresh tube and put on ice to assay the protein concentration. The protein concentration was adjusted with the cell lysis buffer, then the sample (50 μl) was added to twofold concentrated reaction buffer [50 μl; 40 mM *N*-(2-hydroxyethyl)piperazine-*N*′-ethanesulfonic acid, pH 7.4, 3 mM 3-[(3-cholamidopropyl)dimethylammonio]propanesulfonate, 10 mM dithiothreitol, and 4 mM EDTA] and LEHD-pNA (caspase-9) or IEHD-pNA (caspase-8) or DEVD-pNA (caspase-3; 5 μl, 4 mM), then incubated at 37°C for 24 h. After incubation, every sample was read at 405 nm in a Bio-Rad 680 microplate reader.

Selective DNA binding measurements

Fluorescence measurements

Fluorescence measurements (Tan et al. 2007c) were made using a Perkin–Elmer LS-50B fluorescence spectrophotometer with a slit width 5 nm for the excitation and emission beams. Fluorescence titrations were carried out by adding increasing amounts of CT DNA directly to the cell containing the solution of $Ni(Que)_2(H_2O)_2$ complex ($c = 30$ μM, 0.01 M Tris buffer, pH 7.2). To determine the selective binding of the complex to DNA with different sequences, another two kinds of DNA [poly(dA)·poly(dT) and poly(dG)·poly(dC)] were introduced to displace CT DNA (Li et al. 2002). The concentration range of the DNA was 0–60 μM bp. Emission spectra were recorded in the region 330–370 nm using an excitation wavelength of 312 nm.

Molecular modeling

Full geometry optimization of the complex starting at C_{2h} symmetry was carried out with the DFT method at the B3LYP/LanL2DZ level (Foresman and Frisch 1996). Molecular mechanics studies of DNA modeling were preformed using the INSIGHT II package. The structure of decameric DNA duplex 5′-d(CCATTAATGG)$_2$-3′ was built and optimized by molecular mechanics in force field of AMBER and ESFF. The processes of the complex intercalating into DNA were simulated by docking method. The complex intercalated between base group pairs of DNA from the major groove and minor groove, respectively. Initially, the plane of the complex, over against the gap between DNA base pairs, was perpendicular to the axis of DNA helix. The complex was placed at the outside of the DNA double helix, which was defined 0 as intercalation depth. Then geometry optimizations and the energy minimum calculation of the system of the complex intercalating into DNA base pairs were carried out. The complex move 2 Å into DNA base pairs, and geometry optimization and the energy minimum calculation are performed, which were repeated until the complex fully intercalated into DNA or energy of the system was 10 kJ/mol higher than that of the previous step. The interactions of DNA with the complex were examined by comparing the potential energy differences among different binding sites of both minor and major grooves.

Statistical evaluation

The cell assay results shown represent the means ± SD from triplicate experiments performed in a parallel manner unless otherwise indicated. Statistical analyses were performed using an unpaired, two-tailed Student's *t* test. All comparisons are made relative to untreated controls and significance of difference is indicated as * $P < 0.05$ and ** $P < 0.01$.

Results

Cytotoxicity study

The potential antiproliferative effects of $Ni(Que)_2(H_2O)_2$ complex on the viability of tumor cell lines (HepG2, SMMC7721 and A549) were detected by the MTT assay. The concentrations which showed 50% (IC_{50}) inhibition of the cell viability were analyzed by SPSS software and the results are listed in Table 1. From Table 1, the complex significantly inhibits growth and proliferation of all three tumor cells in a dose- and time-dependent manner. The cells showed different sensitivity to the compound with HepG2 cells appearing most sensitive among three cells lines. The viability of HepG2, SMMC7721 and A549 cells was 10.7 ± 0.5, 13.0 ± 0.7 and 16.0 ± 0.8%, respectively, after treatment with 100 μM of $Ni(Que)_2(H_2O)_2$ complex for 48 h. As shown in Table 1, the estimated IC_{50} values of the complex were 14.4 ± 0.9, 19.6 ± 0.6 and 35.6 ± 0.8 μM obtained for 48 h treatment of HepG2, SMMC7721 and A549 cells, respectively, but those of $(Que)_2$ were 33.7 ± 1.0, 42.1 ± 1.0 and 72.1 ± 1.2 μM in the same conditions. The results illustrate that the cytotoxicity of $Ni(Que)_2(H_2O)_2$ complex is much higher than that of quercetin alone.

Table 1 Effect of quercetin and quercetin nickel (II) complex on the viability[a] of tumor cells

Tumor cells	Time (h)	IC_{50} (μmol/l)	
		$(Que)_2$	$Ni(Que)_2(H_2O)_2$
HepG2	24	49.3 ± 1.3	26.0 ± 0.9
	48	33.7 ± 1.0	14.4 ± 0.9
	72	13.3 ± 1.0	6.8 ± 0.3
SMMC 7721	24	63.1 ± 1.2	36.4 ± 0.8
	48	42.1 ± 1.0	19.6 ± 0.6
	72	27.5 ± 1.0	10.9 ± 0.3
A549	24	103.9 ± 1.4	75.8 ± 1.1
	48	72.1 ± 1.2	35.6 ± 0.8
	72	34.9 ± 1.1	13.3 ± 0.4

[a] Cell viabilities were evaluated by MTT assays. Cells were incubated for 0–72 h without (control) or with 0–100 μM of the tested compound. IC_{50} are concentrations which produced 50% inhibition of the cell viability. Results are expressed as means ± SD ($n = 3$)

Apoptosis activity

To further address the death pattern, after treatment with $Ni(Que)_2(H_2O)_2$ complex, HepG2 cells were stained with Hoechst33258 and AO/EB, respectively. The Hoechst33258 staining and AO/EB is sensitive to DNA and was used to assess changes in nuclear morphology. The results of Hoechst33258 staining assay showed that cells demonstrated apoptotic features such as nuclear shrinkage, chromatin condensation, or fragmentation, after treatment with the complex for 24 h. The ratio of cells with a profile of chromatin condensation and fragmented fluorescent nuclei increased in a dose-dependent manner (Fig. 1a).

AO/EB staining combines the differential uptake of fluorescent DNA binding dyes AO and EB and the morphologic aspect of chromatin condensation in the stained nucleus, allowing one to distinguish viable, apoptotic, and necrotic cells. Viable cells possess uniform bright green nucleus. Early apoptotic cells show bright green areas of condensed or fragmented chromatin in the nucleus, and necrotic cells show uniform bright orange nucleus. After staining with AO/EB, the HepG2 cells showed a slight change in cell morphology, with the periphery being very rough and showing effervescence, crumb-like structures, nuclear fragmentation occurred, apoptotic bodies appeared, the permeability of cell membrane increased, and both the window for AO and that for EB stained, which was typical apoptosis characteristic (Fig. 1b).

The apoptotic rate occurred in a dose-dependent manner calculated after Hoechst33258 staining assay. After treatment with 40 μM of $Ni(Que)_2(H_2O)_2$ complex for 24 h, the apoptotic rate of HepG2 cells was 39.2%. In the 80 μM treatment, the apoptotic rate was 52.8% (Fig. 1c).

The expression of survivin, bcl-2 and p53 proteins by immunocytochemistry

We further examined whether $Ni(Que)_2(H_2O)_2$ complex could modulate the expression of survivin, bcl-2 and p53 proteins by immunocytochemistry. After treatment with the complex for 24 h, the levels of survivin and bcl-2 proteins decreased significantly, while the level of p53 protein increased. The levels of survivin, bcl-2 and p53 proteins expression in HepG2 cells were clearly correlated to the concentration of $Ni(Que)_2(H_2O)_2$ complex (Fig. 2, Fig. S1 in Supplementary material).

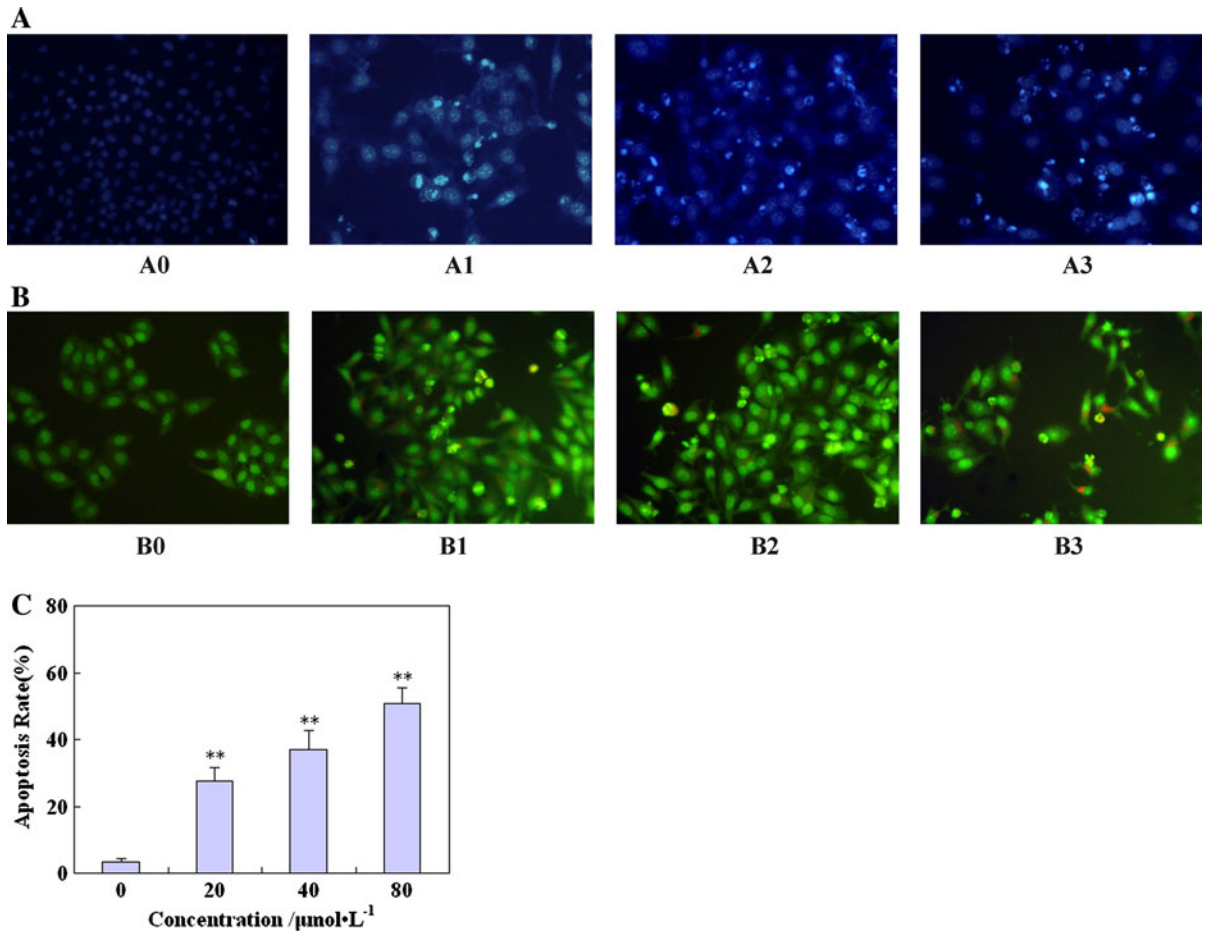

Fig. 1 The morphological changes of HepG2 cells after treatment with quercetin nickel (II) complex as observed under a fluorescent microscope (*A0–A3*, *B0–B3*). **a** Hoechst33258 staining. Cells were treated without the complex (*A0*) or with the complex at 20 μM (*A1*), 40 μM (*A2*) and 80 μM (*A3*) for 24 h. **b** AO/EB staining. Cells were treated without the complex (*B0*) or with the complex at 20 μM (*B1*), 40 μM (*B2*) and 80 μM (*B3*) for 24 h. **c** Apoptotic cells were analyzed. Results are expressed as means ± SD ($n = 3$). * $P < 0.05$, ** $P < 0.01$ compared with control group

The levels of survivin, bcl-2 and p53 proteins expression occurred in a dose dependent manner and were calculated after observed with an optical microscope. After treatment with 60 μM $Ni(Que)_2(H_2O)_2$ complex for 24 h, the levels of survivin and bcl-2 proteins expression in HepG2 cells decreased by 63.6, 54.2%, respectively, while the levels of p53 proteins expression in HepG2 cells increased by 200%.

Activity of caspase-3, 8, 9 by absorption spectroscopy

To demonstrate the molecular mechanisms of apoptosis of HepG2 cells induced by $Ni(Que)_2(H_2O)_2$ complex, we further measured the caspase-3, -8, and -9 activities from absorption spectra. After treatment with 20, 60 μM $Ni(Que)_2(H_2O)_2$ complex for 24 h, relative activity of caspase-3 increased by 222 and 313%, respectively; relative activity of caspase-9 increased by 246 and 335%, respectively. Under the same conditions, however, change in the activity of caspase-8 was not significant (Fig. 3).

Selective DNA binding of $Ni(Que)_2(H_2O)_2$ complex

$Ni(Que)_2(H_2O)_2$ complex can interact with the DNA via an intercalation mode [27]. The fluorescence

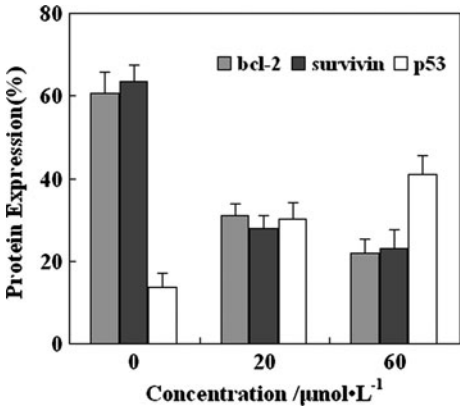

Fig. 2 Effects of quercetin nickel (II) complex on the expression of bcl-2, survivin and p53 proteins in HepG2 cells. HepG2 cells were treated with 0, 20, 60 μM of the complex for 24 h. Results are expressed as means ± SD ($n = 3$). * $P < 0.05$, ** $P < 0.01$ compared with control group

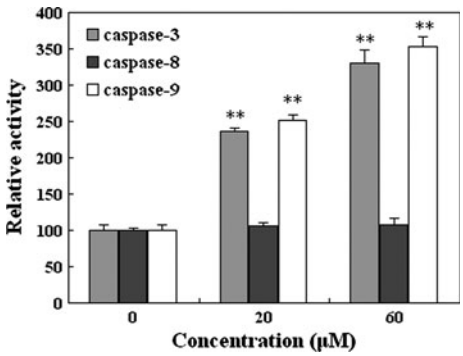

Fig. 3 Caspase-3, -8 and -9 activities in HepG2 cells after treatment with quercetin nickel (II) complex for 24 h. The OD_{405} values were measured and the caspase activity was expressed relative to the untreated control, designated as 100. Results are expressed as means ± SD ($n = 3$). * $P < 0.05$, ** $P < 0.01$ compared with control group

spectra of $Ni(Que)_2(H_2O)_2$ complex, exhibiting a broad emission band in the range 340–360 nm, were monitored at a fixed concentration of 30 μM. Fluorescence intensity increased when CT DNA was added into the complex solution, which may be largely due to the intercalative interaction between adjacent base pairs of CT DNA and the complex. Figure 4 shows the fluorescence intensity of the complex increased when the different kinds of DNA were added into the complex solution. In Fig. 4, I_0 and I represent the fluorescence intensities in the absence or presence of the DNA, respectively. The result illustrates that there is the largest increase in

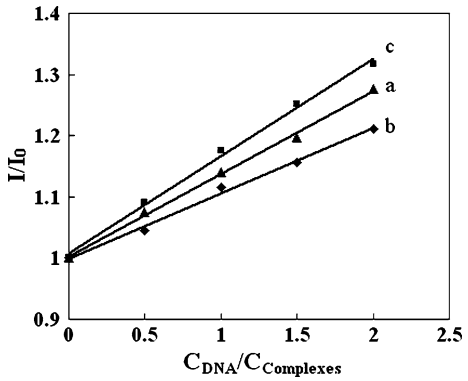

Fig. 4 Effects of CT DNA (*a*), poly(dA)·poly(dT) (*b*) and poly(dG)·poly(dC) (*c*) on relative fluorescence intensity of quercetin nickel (II) complex. The CT DNA, poly(dA)·poly(dT) and poly(dG)·poly(dC) were added into the complex solution, respectively. Emission spectra were recorded in the region 330–370 nm using an excitation wavelength of 312 nm. I_0 and I represent the fluorescence intensities in the absence or presence of the complex, respectively

fluorescence intensity when poly(dG)·poly(dC) is added into the complex solution. So the binding affinity between the complex and poly(dG)·poly(dC) may be larger than that between the complex and CT DNA (or the poly(dA)·poly(dT)).

The modeling results were tabulated in Table 2, which shows the change of total potential energies of the process of $Ni(Que)_2(H_2O)_2$ complex docking between DNA base pairs from major and minor groove. From the table, total potential energies of complex–DNA binding system after intercalation, are much less than those of the system before intercalation, which may be associate with electrostatic interaction and space matching. Furthermore, total potential energy of complex–DNA binding system formed by complex intercalating into C5G6 region from minor groove is less than those of other systems, illustrating that the minor groove binding of the complex in C5G6 region is the most preferential binding modeling of the interactions between the complex and DNA base pairs, which agrees with the above result of fluorescence measurement.

Discussion

In recent years, previous reports have been shown that quercetin metal complexes could interact with

Table 2 Total potential energies (kJ/mol) of intercalation of quercetin nickel (II) complex into DNA base pairs

Insert depth (Å)	Minor groove					Major groove				
	G3T4	T4C5	C5G6	G6A7	A7C8	G3T4	T4C5	C5G6	G6A7	A7C8
0	2680.01	2700.96	2693.04	2685.38	2709.30	2711.05	2694.94	2714.16	2697.08	2692.60
2	2619.93	2616.68	2606.06	2610.59	2653.41	2656.02	2637.09	2659.40	2631.95	2621.83
4	2588.18	2571.83	2565.84	2567.13	2617.51	2611.62	2608.35	2629.52	2597.69	2572.90
6	2551.82	2529.67	2519.80	2524.64	2592.59	2579.04	2575.00	2601.59	**2562.55**	**2525.04**
8	**2511.96**	2491.31	2477.20	**2485.33**	**2583.84**	2550.27	**2560.44**	2576.27	2576.75	2538.42
10	2522.05	**2464.80**	**2446.73**	2502.86	2598.96	**2530.23**	2573.30	**2565.53**	2587.51	2547.32

Bold value is the minimum value among each row of data

DNA via an intercalative mode, and furthermore induce cancer cell apoptosis (Tan et al. 2007a, b, 2009a, b, c). There is a lack of evidence to support the relationship between DNA binding properties of $Ni(Que)_2(H_2O)_2$ complex and its apoptosis-induced activity.

In the present study, we found that $Ni(Que)_2(H_2O)_2$ complex induced the cell growth inhibition and apoptosis in cancer cells. The complex has a significant inhibition to growth and proliferation of HepG2, A549 and SMMC7721 cells in a dose- and time-dependent manner. After treatment with $Ni(Que)_2(H_2O)_2$ complex, HepG2 cells stained with Hoechst33258 were characterized by nuclear shrinkage, chromatin condensation, or fragmentation (Fig. 2). This suggested that HepG2 cells underwent the typical morphologic changes of apoptosis after exposure to $Ni(Que)_2(H_2O)_2$ complex.

To clarify the mechanisms of cell apoptosis induced by $Ni(Que)_2(H_2O)_2$ complex, we detected the levels of survivin, bcl-2 and p53 proteins in HepG2 cells treated with $Ni(Que)_2(H_2O)_2$ complex. Survivin, a member of apoptosis inhibitor family, is expressed in most human malignancies and implicated in mitosis regulation and preservation of cell viability (Badran et al. 2004). Previous studies have demonstrated that survivin is essential for cell cycle progression in hepatocellular carcinoma cells, and down regulation of survivin expression may lead to programmed cell death (Ito et al. 2000), indicating that survivin may be an appealing new target for novel therapies in hepatocellular carcinoma (Moon and Tarnawski 2003). Otherwise, it has been proposed that bcl-2 over-expression could delay or prevent the action of a wide variety of cell apoptosis (Yang et al. 1997). In the present study, we found that the levels of survivin and bcl-2 proteins decreased, while the levels of p53 protein increased in the HepG2 cell after treatment with $Ni(Que)_2(H_2O)_2$ complex. Our results indicate that bcl-2 may be transcriptionally down-regulated by p53, and then promote cell apoptosis. Meanwhile, the level of survivin is negatively correlated to that of p53, which may be result from enhanced expression of p53 protein (Kuo et al. 2004). Further data demonstrated that the activities of caspase-3 and caspase-9 in the HepG2 cell were elevated after treatment with $Ni(Que)_2(H_2O)_2$ complex, while activity of caspase-8 was no change. Therefore, it was suggested that mitochondria may play a more important role than death receptors in the HepG2 cells apoptosis induced by $Ni(Que)_2(H_2O)_2$ complex.

What is more, the results from fluorescence measurements and molecular modeling illustrated that $Ni(Que)_2(H_2O)_2$ complex could preferentially bind to the CG-rich sequences of DNA. It has been reported that some compounds, such as mithramycin and hedamycin, preferentially binding to GC-rich DNA are able to block overactive transcription factors and modulate gene expression, which could be very attractive therapeutic agents (Sastry and Patel 1993; Wu et al. 2005). In particular, survivin and bcl-2 genes possess the GC-rich sequences (GC-box) which play a vital role in their basal transcription. It has been demonstrated that the specific interactions of Sp1 or Sp1-like proteins with the cis-acting DNA elements in GC-rich human survivin promoter are of great importance for its basal transcription, and that the inhibition of these interactions by the anticancer agent could result in the down regulation of survivin gene transcription (Wu et al. 2005) [7]. On the basis of above experimental results, we demonstrated that $Ni(Que)_2(H_2O)_2$ complex may intercalate into the

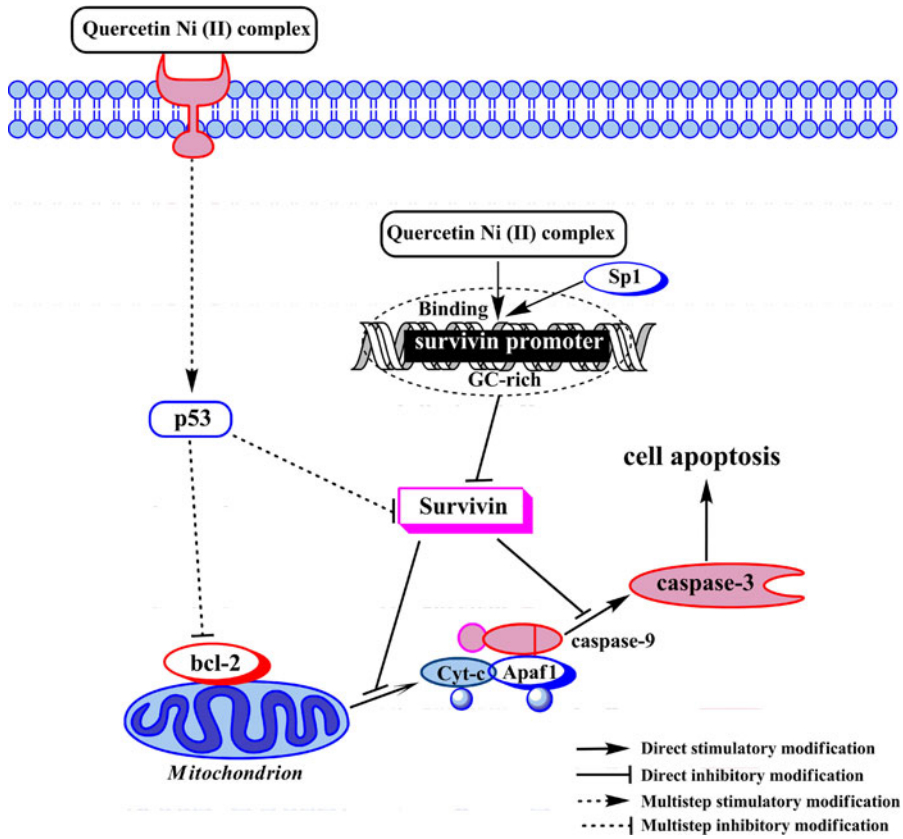

Fig. 5 Proposed mechanism of HepG2 cells apoptosis induced by quercetin nickel (II) complex

GC-rich core promoter region of survivin and competitively inhibit the binding of Sp1 protein to CG-rich sequences in gene promoter (Fig. 5), down-regulating survivin gene expression and promoting tumor cells apoptosis, like hedamycin (Wu et al. 2005).

In conclusion, we have uncover the selective intercalation binding modes of $Ni(Que)_2(H_2O)_2$ complex with DNA involved in the cytotoxicity of the complex. The finding shows that sequence-selective DNA binding of the complex could play an important but not exclusive role in its antitumor activity. Moreover, the antitumor activity of $Ni(Que)_2(H_2O)_2$ complex could be attributed at least in part to their ability to interact with GC-rich DNA sequences and interfere with Sp1 or other DNA-binding proteins, resulting in down-regulation of survivin gene. So metal complexes selective binding to GC-rich survivin promoter may be a promising cancer therapeutic agent.

Acknowledgments This work was financially supported by National Natural Science Foundation of China (No. 20901086), China Postdoctoral Science Foundation funded project (No. 20090450788), and the Fundamental Research Funds for the Central Universities (No. CDJRC10230002).

References

Albertini V, Jain A, Vignati S, Napoli S, Rinaldi A, Kwee I, Nur-e-Alam M, Bergant J, Bertoni F, Carbone GM, Rohr J, Catapano CV (2006) Novel GC-rich DNA-binding compound produced by a genetically engineered mutant of the mithramycin producer *Streptomyces argillaceus* exhibits improved transcriptional repressor activity: implications for cancer therapy. Nucleic Acids Res 34:1721–1734

Altieri DC (2001) The molecular basis and potential role of survivin in cancer diagnosis and therapy. Trends Mol Med 7:542–547

Asadi M, Safaei E, Ranjbar B, Hasani L (2004) Thermodynamic and spectroscopic study on the binding of cationic Zn(II) and Co(II) tetrapyridinoporphyrazines to calf thymus DNA: the role of the central metal in binding parameters. New J Chem 28:1227–1234

Badran A, Yoshida A, Ishikawa K, Goi T, Yamaguchi A, Ueda T, Inuzuka M (2004) Identification of a novel splice variant of the human anti-apoptopsis gene survivin. Biochem Biophys Res Commun 314:902–907

Foresman JB, Frisch AE (1996) Exploring chemistry with electronic structure methods, 2nd edn. Gaussian Inc, Pittsburgh

Gao F, Chao H, Zhou F, Chen X, Wei YF, Ji LN (2008) Synthesis, GC selective DNA binding and topoisomerase II inhibition activities of ruthenium(II) polypyridyl complex containing 11-aminopteridino[6,7-f][1,10]phenanthrolin-13(12H)-one. J Inorg Biochem 102:1050–1059

Hecht SM (2000) Bleomycin: new perspectives on the mechanism of action. J Nat Prod 63:158–168

Ito T, Shiraki K, Sugimoto K, Yamanaka T, Fujikawa K, Ito M, Takase K, Moriyama M, Kawano H, Hayashida M, Nakano T, Suzuki A (2000) Survivin promotes cell proliferation in human hepatocellular carcinoma. Hepatology 31:1080–1085

Koutsodontis G, Kardassis D (2004) Inhibition of p53-mediated transcriptional responses by mithramycin A. Oncogene 23:9190–9200

Kožurková M, Sabolová D, Janovec L, Mikes J, Kovaľ J, Ungvarský J, Stefanisinová M, Fedorocko P, Kristian P, Imrich J (2008) Cytotoxic activity of proflavine diureas: synthesis, antitumor, evaluation and DNA binding properties of 1′,1″-(acridin-3,6-diyl)-3′,3″-dialkyldiureas. Bioorg Med Chem 16:3976–3984

Kuo PC, Liu HF, Chao JL (2004) Survivin and p53 modulate quercetin-induced cell growth inhibition and apoptosis in the human lung carcinoma cells. J Biol Chem 279:55875–55885

Li WY, Zhu ST, He XW (2002) Study on the interaction mechanism between Ge-132 and DNA by spectral methods. Acta Chim Sin 60:105–108

Metcalfe C, Thomas JA (2003) Kinetically inert transition metal complexes that reversibly bind to DNA. Chem Soc Rev 32:215–224

Moon WS, Tarnawski AS (2003) Nuclear translocation of Survivin in hepatocellular carcinoma: a key to cancer cell growth? Hum Pathol 34:1119–1126

Mosmann T (1983) Rapid colorimetric assay for cellular growth and survival: application to proliferation and cytotoxicity assays. J Immunol Methods 65:55–63

Navarro M, Cisneros-Fajardo EJ, Sierralta A, Fernández-Mestre M, Silva P, Arrieche D, Marchán E (2003) Design of copper DNA intercalators with leishmanicidal activity. J Biol Inorg Chem 8:401–408

Ray R, Thomas S, Miller DM (1990) Mithramycin selectively inhibits the transcriptional activity of a transfected human c-myc gene. Am J Med Sci 300:203–208

Remsing LL, Bahadori HR, Carbone GM, McGuffie EM, Catapano CV, Rohr J (2003) Inhibition of c-src transcription by mithramycin: structure-activity relationships of biosynthetically produced mithramycin analogues using the c-src promoter as target. Biochemistry 42:8313–8324

Sastry M, Patel DJ (1993) Solution structure of the mithramycin dimer–DNA complex. Biochemistry 32:6588–6604

Sastry M, Fiala R, Patel DJ (1995) Solution structure of mithramycin dimers bound to partially overlapping sites on DNA. J Mol Biol 251:674–689

Sheng X, Guo X, Lu XM, Lu GY, Shao Y, Liu F, Xu Q (2008) DNA binding, cleavage, and cytotoxic activity of the preorganized dinuclear zinc(II) complex of triazacyclononane derivatives. Bioconjug Chem 19:490–498

Silvestri A, Barone G, Ruisi G, Lo Giudice MT, Tumminello S (2004) The interaction of native DNA with iron(III)-N,N′-ethylene-bis(salicylideneiminato)-chloride. J Inorg Biochem 98:589–594

Song YM, Wu Q, Yang PJ, Luan NN, Wang LF, Liu YM (2006) DNA Binding and cleavage activity of Ni (II) complex with all-trans retinoic acid. J Inorg Biochem 100:1685–1691

Tan J, Wang BC, Zhu LC (2007a) Hydrolytic cleavage of DNA by quercetin zinc(II) complex. Bioorg Med Chem Lett 17:1197–1199

Tan J, Wang BC, Zhu LC (2007b) Hydrolytic cleavage of DNA by quercetin manganese(II) complex. Colloid Surf B 55:149–152

Tan JH, Lu YJ, Huang ZS, Gu LQ, Wu JY (2007c) Spectroscopic studies of DNA binding modes of cation-substituted anthrapyrazoles derived from emodin. Eur J Med Chem 42:1169–1175

Tan CP, Liu J, Chen LM, Shi S, Ji LN (2008) Synthesis, structural characteristics, DNA binding properties and cytotoxicity studies of a series of Ru (III) complexes. J Inorg Biochem 102:1644–1653

Tan J, Wang BC, Zhu LC (2009a) DNA binding, cytotoxicity, apoptotic inducing activity and molecular modeling study of quercetin zinc (II) complex. Bioorg Med Chem 17:614–620

Tan J, Wang BC, Zhu LC (2009b) DNA binding and oxidative DNA cleavage induced by quercetin copper (II) complex: potential mechanism of its antitumor properties. J Biol Inorg Chem 14:727–739

Tan J, Wang BC, Zhu LC (2009c) DNA binding and cleavage activity of quercetin nickel (II) complex. Dalton Trans 7:4722–4728

Wu JG, Ling X, Pan DL, Apontes P, Song L, Liang P, Altieri DC, Beerman T, Li FZ (2005) Molecular mechanism of inhibition of survivin transcription by the GC-rich sequence-selective DNA binding antitumor agent, hedamycin—evidence of survivin downregulation associated with drug sensitivity. J Biol Chem 280:9745–9751

Xu H, Zheng KC, Deng H, Lin LJ, Zhang QL, Ji LN (2003a) Effects of ligand planarity on the interaction of polypyridyl Ru(II) complexes with DNA. Dalton Trans 3:2260–2268

Xu H, Zheng KC, Deng H, Lin LJ, Zhang QL, Ji LN (2003b) Effects of the ancillary ligands of polypyridyl ruthenium(II) complexes on the DNA-binding behaviors. New J Chem 27:1255–1263

Yang J, Liu X, Bhalla K, Kim CN, Ibrado AM, Cai J, Peng TI, Jones DP, Wang X (1997) Prevention of apoptosis by Bcl-2: release of cytochrome c from mitochondria blocked. Science 275:1129–1132

Zhang H, Liu CS, Bu XH, Yang M (2005) Synthesis, crystal structure, cytotoxic activity and DNA-binding properties of the copper (II) and zinc (II) complexes with 1-[3-(2-pyridyl)pyrazol-1-ylmethyl]naphthalene. J Inorg Biochem 99:1119–1125

Zuber G, Quada JC Jr, Hecht SM (1998) Sequence selective cleavage of a DNA octanucleotide by chlorinated bithiazoles and bleomycins. J Am Chem Soc 12:9368–9369